Research Paper

Journal of Engineering and Technological Sciences

The Risk of Failure Assessment in Bina Marga Standard Designed Prestressed Concrete Girder Bridges under B-WIM Load Measurement

Widi Nugraha[1,2,*], Indra Djati Sidi[1], Made Suarjana[1] & Ediansjah Zulkifli[1]

[1]Department of Civil Engineering, Institut Teknologi Bandung, Jalan Ganesha No. 10, Bandung 40132, Indonesia
[2]Directorate General of Highway, Ministry of Public Works and Housing, Jalan AH Nasution No. 264, Bandung 40294, Indonesia

Corresponding author: widi.nugraha@pu.go.id

Abstract

The use of precast prestressed concrete girder bridges in Indonesia has been increasing rapidly due to their high quality, reliability, and faster construction on site. The girder components are typically designed for a specific bridge span and can be prefabricated. The Directorate General of Highways of the Ministry of PUPR (Bina Marga) has released a standard design for prestressed concrete girder bridges with a typical span of up to 40 m. This design is based on the bridge loading standard SNI 1725 2016, which determines the live traffic load through consensus due to limited data on actual traffic load measurement results. However, the Ministry of PUPR has been implementing actual traffic load measurements using weigh-in-motion (WIM) technology to directly measure the load of passing vehicles. In this study, a risk assessment of the failure risk of a standard Bina Marga bridge with a 40-m span prestressed concrete girder type was conducted based on B-WIM load measurements. The results of this assessment indicate that the standard Bina Marga bridge has a failure risk of 1.48 x 10-4, which is smaller than the acceptable risk of failure according to the AASHTO LRFD Bridge Design Specification as referenced in SNI 1725 2016.

Keywords: *B-WIM; failure risk assessment; live traffic load; precast prestressed concrete girder bridges, reliability.*

Introduction

Bridges are essential structures that connect different regions and facilitate transportation and mobility. They are designed to support and carry traffic loads using various materials, such as wood, masonry, reinforced concrete, steel, and prestressed concrete. Among these materials, prestressed concrete has become increasingly popular in bridge construction due to its advantages over conventional reinforced concrete. Prestressed concrete structures optimize the use of high concrete strength against compressive forces by applying a pre-tensioning force to steel cables embedded in the lower part of the cross section. This creates a compressive stress that counteracts the tensile stress induced by bending forces from traffic loads, allowing for smaller cross sections and longer spans than ordinary reinforced concrete structures. Notably, this prestress force also exerts a positive influence on critical structural aspects like the fundamental frequency and static deflection shape of girders, ultimately enhancing performance when compared to their reinforced concrete counterparts [1]. Moreover, prestressed concrete girders can be prefabricated off-site with a typical design for the same span length, leading to faster construction compared to reinforced concrete girders that are cast on site [2]. Prestressed concrete girder bridges have been widely used around the world for various types of bridges, such as box girder bridges (e.g., Shibanpo Yangtze Bridge in China), T-girder bridges (e.g., Stolma Bridge in Norway), or I-girder bridges (e.g., Natchez Trace Parkway Arches in USA).

However, despite their benefits, prestressed concrete girder bridges also face challenges, with deterioration being a primary concern [3]. The degradation of these structures is attributed to a combination of factors, including prestressing losses, tendon relaxation, concrete cracking, concrete creep and shrinkage, and the influence of environmental factors [4]. A particularly noteworthy concern is the occurrence of cracking, which

ISSN: 2337-5779
J. Eng. Technol. Sci. Vol. 55, No. 5, 2023, 558-568
DOI: 10.5614/j.eng.technol.sci.2023.55.5.5

DOI: 10.5614/j.eng.technol.sci.2023.55.5.5

has the potential to significantly erode the flexural stiffness of the girder [5]. This, in turn, can lead to a reduction in both static and dynamic performance, adversely affecting the bridge's capacity to bear various loads. Therefore, it is important to evaluate their performance and safety using reliable methods that account for their structural characteristics and loading conditions, including live traffic loads, seismic forces, wind pressures, and more. Through a comprehensive evaluation of the risk of failure, proactive measures can be implemented to ensure that the risk aligns with established safety thresholds. This may entail updates to the loading regulations in Indonesia's bridge design code (SNI) [6]. The existing Indonesia bridge design code (SNI) operates in accordance with the principles of Load and Resistance Factor Design (LRFD), employing a risk-based and probabilistic approach to define crucial provisions, including nominal loading and load factors [7].

In this paper, we focus on prestressed concrete girder bridges in Indonesia and their loading conditions. In Indonesia, the Bina Marga standard design for prestressed bridges with spans ranging from 22 m to 40 m [8] is based on the bridge loading code SNI 1725 2016 [9]. However, the SNI 1725 2016 determines the amount of live traffic load through consensus by referencing foreign bridge loading standards, such as those from the United States (AASHTO LRFD Bridge Design Specifications [10]) and Australia (Bridge Management System [11]), rather than actual vehicle measurement data. Using actual vehicle measurement data can provide more realistic and accurate estimates of the load effects and risk of failure of bridges under different traffic scenarios. One option is to use weigh-in-motion (WIM) technology to measure the actual vehicle loads on Indonesian bridges. WIM technology is constantly evolving, with various types of pavement-based WIM and bridge WIM (B-WIM) sensors currently available [12]. In Indonesia, the Ministry of PUPR has started measuring actual vehicle loads with B-WIM in recent years. B-WIM measurement stations have been operating on the North Coast of Central Java national road section since 2017 and have also been installed at several other locations on national roads and toll roads [13]. The data generated from B-WIM measurements includes the total vehicle load, the weight of individual axles, the distance between the axles, the vehicle speed, the axle configuration, and the time the vehicle passes [14]. However, B-WIM data also pose some challenges for bridge analysis, such as data quality issues, calibration errors, environmental influences, or sensor failure [15]. These challenges need to be addressed in order to use B-WIM data effectively for risk assessment of prestressed concrete girder bridges.

The objective of this study was to develop a comprehensive risk assessment method for prestressed concrete girder bridges utilizing data from bridge weigh-in-motion (B-WIM) systems to enhance structural analysis models. To achieve this, we utilized B-WIM data obtained from a measurement station situated along a national road in Central Java, which has been in operation since 2017, as illustrated in Figure 1.

Figure 1 B-WIM instrumentation on the PCI girder bridge.

To align with best practices, we adopted a standard B-WIM system sensor layout designed for both girder and slab bridges, depicted in Figure 2. Within this layout, strategically positioned strain transducers were affixed at the mid span of each girder's bottom flange, denoted by the red rectangles. These strain gauges played a crucial role in capturing the maximum strain induced by vehicles passing over the bridge, effectively functioning as weighing sensors for the B-WIM measurement system. Additionally, the strain transducers also served as speed and axle detection sensors, installed at the bottom part of the slab in each vehicle lane, as indicated by the black rectangles. All these sensors were interconnected with a data processing unit, depicted by the gray rectangle, dedicated to processing the bridge response data from the sensors and calculating essential B-WIM output parameters such as vehicle gross vehicle weight (GVW), axle load, axle distance, speed, and classification, using the Moses algorithm [16].

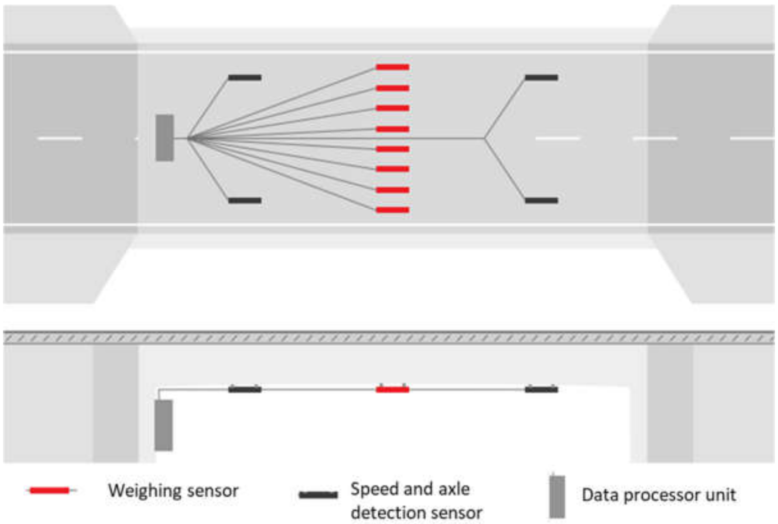

Figure 2 Typical B-WIM system installation [17].

We applied statistical methods to extract the characteristic values and distributions of the vehicle parameters from the B-WIM data. We then selected a set of representative load cases that cover different combinations of vehicle types, weights, speeds, and positions on the bridge. The simulation involved applying moving loads on a standard Bina Marga prestressed concrete girder bridge model to determine the response of the prestressed concrete girder elements to actual traffic loads. The response of the structure can vary due to different load and vehicle configurations, resulting in a random variable response distribution. In addition to the response variable due to load, the resistance of the prestressed concrete girder to external loads is also a random variable because the forming materials, such as concrete, steel strands, and reinforcing steel, are themselves random variables. Therefore, there is a risk of failure if the response of the structure to loading exceeds the bearing capacity of the structure. This study analyzed and evaluated the risk of failure against an acceptable target risk of structural failure based on the importance of the bridge infrastructure according to the SNI code in Indonesia [9]. We expected our method to provide more realistic and accurate estimates of the load effects and risk of failure of prestressed concrete girder bridges under actual traffic scenarios than conventional methods based on design codes. Our method could also help to identify critical load cases and locations on the bridge that require more attention. Furthermore, our method can be applied to other types of bridges or WIM data sources with minor modifications.

Standard Design for Prestressed Concrete Girder Bridge

In 2008, the Directorate General of Highways released a standard design for prestressed concrete girder bridges with a cross section in the shape of type I beams and spans ranging from 22 m to 40 m. The bridge analyzed in this study has a 40 m span with a traffic width of 7 m and sidewalks 1 m wide on both sides. Figure 3 provides an in-depth view of the dimensions and section specifics of this standardized design. The girders used are 2300

DOI: 10.5614/j.eng.technol.sci.2023.55.5.5

mm x 850 mm with a total of five girders arranged with a distance of 1750 mm between them. These girders are connected with locally cast diaphragms measuring 200 mm x 1850 mm at intervals of 10 m, 20 m, and 30 m from the initial supports. The structural components utilize a mix of materials, including concrete girders with a compressive strength, fc', of 40 MPa, concrete diaphragms, and slabs with a compressive strength fc' of 30 MPa. Reinforcement comprises BJTD40 steel and prestressed PC strands measuring 12.7 mm in diameter, adhering to ASTM-416 Low Relaxation specifications. These detailed specifications were instrumental in modeling the bridge using the 3D finite element method (FEM) and accurately calculating the bridge's resistance or capacity. It is noteworthy that the material strength values presented herein are nominal and they were further converted to mean values using bias factors, subsequently facilitating precise girder resistance calculations essential for reliability analysis.

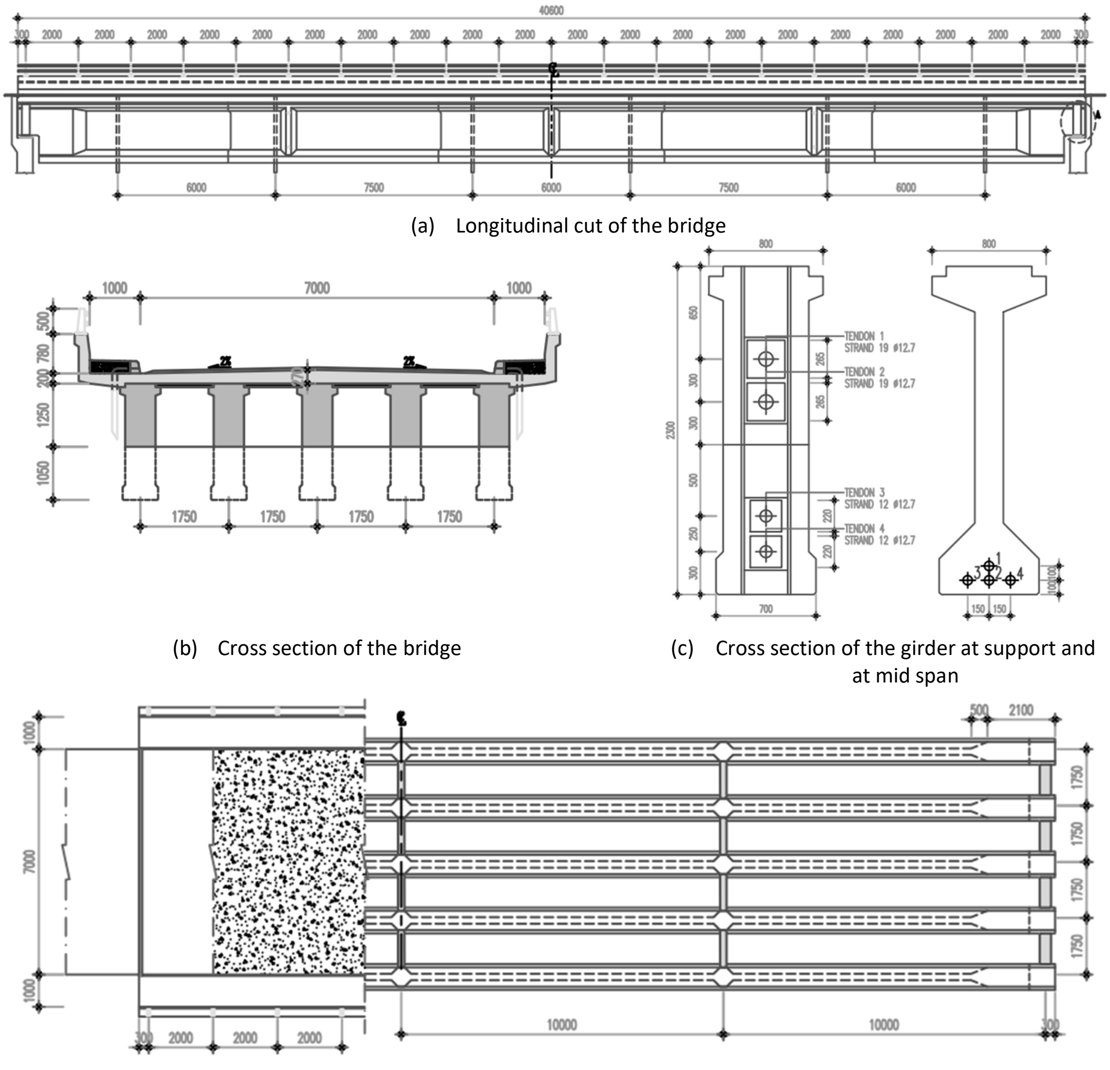

(a) Longitudinal cut of the bridge

(b) Cross section of the bridge

(c) Cross section of the girder at support and at mid span

(d) Plan view of the bridge

Figure 3 Design drawing of 40 m PCI girder bridge.

In the calculation of the resistance variable, we adopted a calculation approach for the PCI girder bending moment capacity under ultimate conditions. This calculation method involves utilizing the principles of force and moment equilibrium, taking into consideration the concrete compressive strength, the tensile strength of the reinforcement bars, and the effect of the prestress force acting on the girder. By integrating these factors, we were able to derive a comprehensive understanding of the girder's capacity to withstand bending moments.

Notably, throughout these calculations, the mean values of material strength and dimensions were employed to ensure accuracy and reliability in the determination of the resistance variable.

To analyze the load effect variable of the standard design for prestressed concrete girder bridges due to bridge WIM live load, a 3D FEM was created using the CSI Bridge Software [18] based on the bridge design drawing and material specification. The FE model was used to simulate traffic loads and calculate the load effect generated by the traffic load simulation. This load effect variable assessment was based on real-world B-WIM vehicle load measurement data, encompassing comprehensive vehicle specifics such as total weight, individual axle weights, axle distances, and axle configurations. The FE model, utilized for the traffic load simulation, is visually presented in Figure 4.

The FE model of the PCI girder bridge consisted of several components, as listed in Table 1. The girder, the primary load-bearing element, was represented using beam/frame elements made of precast concrete with a mesh size of 5 m. Notably, the girder exhibits a non-prismatic geometric characteristic, transitioning from a nearly full section at the support points (measuring 800 x 2300 mm) to a more I-shaped section at mid-span, with an end section length of 2100 mm and a 500-mm transition zone towards the mid-span section, as illustrated in Figure 3(d). Tendons, essential for prestressing, were simulated as tendon elements comprising steel strand material. The prestressing force is applied through pre-tensioning, a process where prestressing tendons, modeled as tendon elements with a curved geometry, are perfectly bonded to the concrete beam. The simulation accurately transfers the prestressing force from the tendon to the concrete reference axis, allowing for the effects of prestressing in the FE model. The slab, supporting the road surface, was simulated using shell-thin elements made of reinforced concrete, with a mesh size of 5 by 0.25 m. Diaphragms, enhancing the structural stability, were represented with reinforced concrete beam/frame elements and a mesh size of 1.75 meters. The boundary conditions applied were of a simple support nature, where one end was designed as a rolled support, and the other as a pin support. Importantly, this study did not delve into geometric nonlinear analyses; it assumes the bridge operates within typical traffic load conditions. These elements, along with their specific mesh sizes, collectively constitute the FE model, enabling a comprehensive analysis of the PCI girder bridge's structural behavior under varying vehicular loads based on B-WIM measurements.

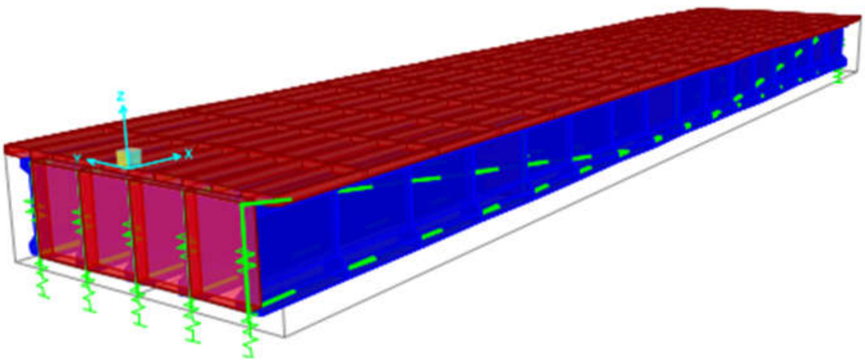

Figure 4 FE Model of 40 m PCI girder bridge.

Table 1 FE model element information.

Element Name	Element type	Material	Mesh Size
Girder	Beam/frame	Precast Concrete	5 m
Tendon	Tendon	Steel Strand	-
Slab	Shell – thin	Reinforced Concrete	5 m x 0.25 m
Diaphragm	Beam/frame	Reinforced Concrete	1.75 m

B-WIM Vehicle Live Load Measurement Data

The data used in this study were based on the results of measuring vehicle loads with B-WIM on the national road along the north coast of Central Java within one year, 2018. Detailed vehicle data, including the time the

DOI: 10.5614/j.eng.technol.sci.2023.55.5.5

vehicle passed, the total weight of the vehicle, the weight of each vehicle axle, the distance between vehicle axles, and vehicle axle configurations, could be obtained from B-WIM measurements. In this study, the data was used to construct a vehicle load sequence for simulating traffic loading on the bridge model. One of the vehicle load sequences with the largest vehicle load effect for a 40-m bridge span was recorded on 2 December 2018, as shown in Figure 5 below. The vehicle sequence was used as a moving load in the bridge structure model to then carry out a loading simulation. Simulations were carried out for other vehicle sequences according to the results of the vehicle load measurements with B-WIM in this study, namely for one year. The output of the model structure analysis were the internal forces in the form of the bending moments and shear of the girder. The maximum internal force value for each daily data from vehicle load measurement results with B-WIM was then recapitulated and the type of variable distribution was sought for the purpose of reliability analysis.

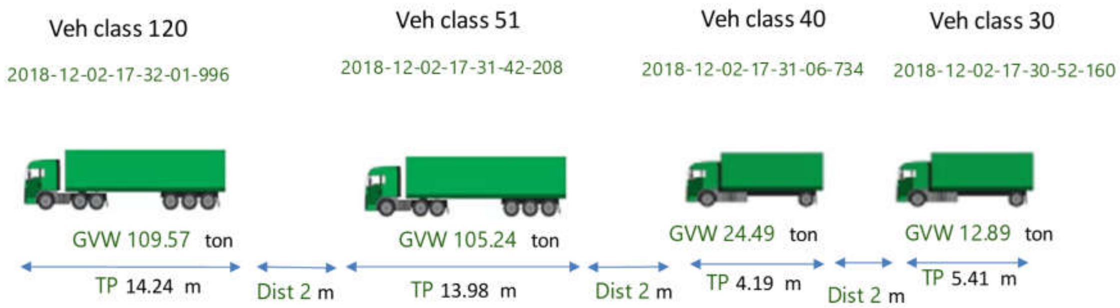

Figure 5 Heaviest 40-m vehicle sequence of 2 December 2018.

The distribution of daily maximum load effects was used to estimate the maximum load effects for a bridge lifespan of 75 years. Since the daily maximum value represents the highest value for that day, it can be assumed that the distribution of daily maximum values follows an extreme value distribution. This study assumed that the daily maximum value follows a Gumbel Type I distribution. Figure 6 shows the projection of the maximum load effects for a 75-year return period.

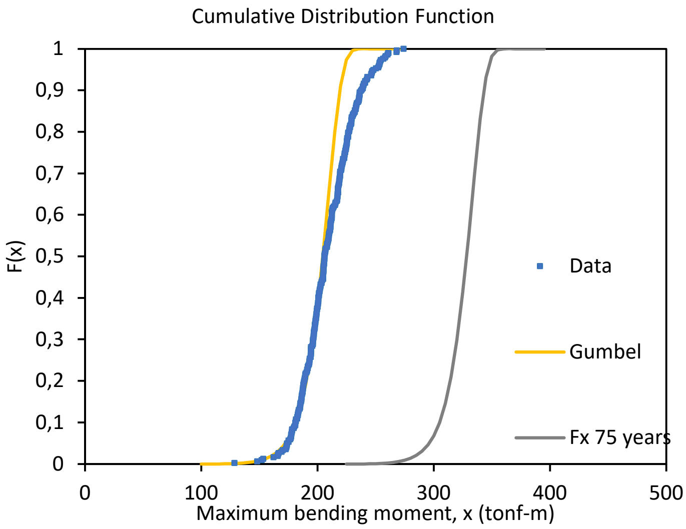

Figure 6 CDF of 75 years maximum bending moment.

Reliability Analysis

Reliability analysis is a method that plays a vital role in determining the risk of failure of a structure. It provides a precise estimate of the probability that the structure will be able to resist the loads it is subjected to over its service life. The primary objective of reliability analysis is to ensure that the structure meets the safety requirements and complies with the codes and standards set by regulatory bodies. The reliability index is the metric used to determine the safety of the structure, and it is calculated by comparing the strength of the structure to the load it is expected to carry. If the reliability index is less than a certain target reliability, the structure may be at risk of failure, and appropriate measures may need to be taken to improve its safety. In this study, the reliability analysis was performed using the first-order reliability method (FORM), a widely accepted and accurate approach for estimating the probability of failure of a structure [19]. FORM is a computational approach utilized to assess the probability of failure within a structure. This probability is typically depicted graphically through a reliability index curve, as illustrated in Figure 7. The figure showcases a probability density function (PDF) of a performance function g, a function influenced by random variables, representing the relationship between resistance R and total loads Q acting on the structure. In essence, the structure is considered safe when the total load Q is less than the resistance R (R > Q), resulting in a positive g value. Conversely, failure occurs if the total load Q surpasses the resistance R (R < Q), leading to a negative g value. The probability of failure (p_f) is calculated based on the area where the distribution of g falls to the left of the y = 0 axis, while the probability of safety (p_s) is computed as 1 - p_f. Additionally, the reliability index β is the inverse of the normal distribution of p_s. These parameters collectively help in comprehensively evaluating the structural safety and failure probability, aiding in effective risk assessment and mitigation strategies.

The load placed on a bridge by vehicles is a random variable, meaning it can vary greatly from one moment to the next. At times, this load may be so large that it exceeds the designed capacity or resistance of the bridge, putting it at risk of failure. This is a concern, because the strength of a bridge must be able to withstand the loads it is subjected to in order to remain safe and functional. If the load on the bridge is consistently too high, the structure may eventually become overloaded and fail, leading to costly repairs or even collapse. To mitigate this risk, it is important to carefully consider the expected loads on a bridge during the design process and ensure that the structure is capable of handling them. Reliability analysis can be used to evaluate the risk of failure of a bridge due to vehicle loads and identify any potential weaknesses or vulnerabilities in the structure.

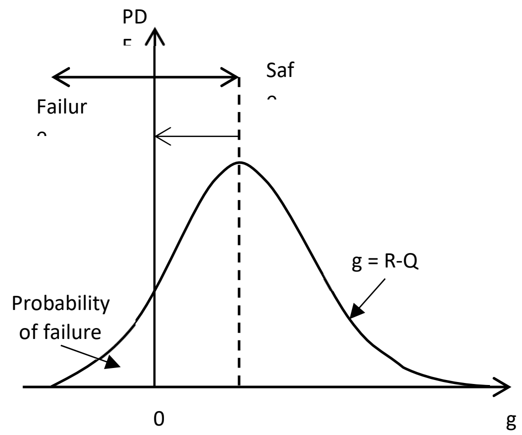

Figure 7 Probability of failure concept.

The risk of failure assessment method used in this study followed the flowchart depicted in Figure 8. The methodology involved utilizing the FE model of the bridge, incorporating Bridge Data to accurately calculate load effects resulting from vehicle loading based on B-WIM measurements. The daily vehicle data was used to construct a vehicle load model, representing one or several vehicles as moving loads on the FE model. Subsequently, the maximum load effect, specifically the maximum bending moment, was computed for each date of the B-WIM measurements data. This process was repeated for each date over a year, allowing statistical data on the daily maximum load effect to be collected. These statistics are pivotal in calculating the 75-year return period of the maximum load effect, a crucial component for the subsequent reliability analysis.

DOI: 10.5614/j.eng.technol.sci.2023.55.5.5

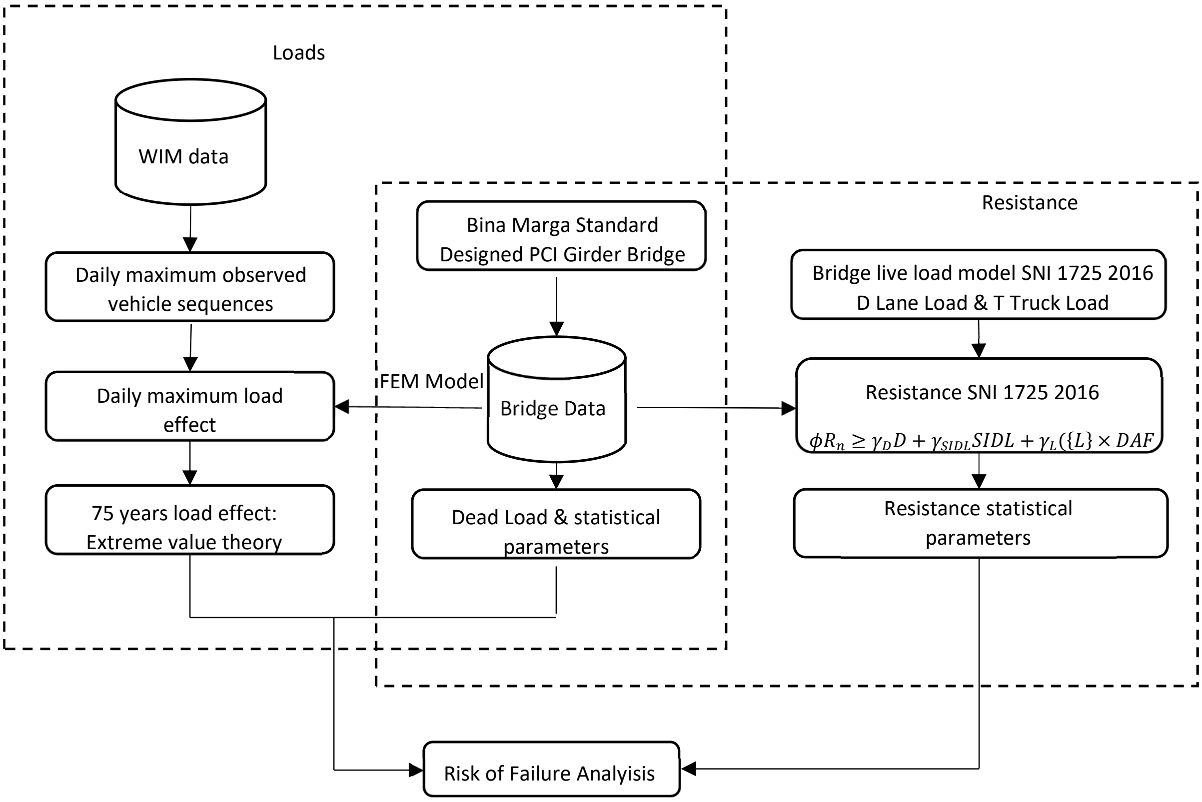

Figure 8 Flowchart for risk of failure analysis.

The mean and standard deviation of the maximum live load effect over a 75-year period were determined using the scale and location parameters, the daily maximum value followed a Gumbel Type I distribution based on distribution fitting. The dead load effect was assumed to follow a normal distribution [20], and the resistance was calculated using the bias factor and coefficient of variation. The reliability index was determined utilizing the First Order Reliability Method (FORM), a widely acknowledged approach represented by Eq. (1). Additionally, the Rosenblatt transformation [21], was applied due to the non-normal distribution of the variables. In this study, the probability distributions for various factors were determined to facilitate reliability analysis. The maximum load effect, representing bending moments, was found to follow a Gumbel Type I distribution through fitting the data, illustrated in Figure 6. Conversely, the dead load effect was assumed to conform to a normal distribution, a standard assumption [22]. To assess the resistance, representing the structure's capacity, careful consideration of its bias factor and coefficient of variation was made. The resistance was modeled using a lognormal distribution, a choice also grounded in previous work [22]. To ensure the reliability analysis was conducted effectively, the Rosenblatt transformation was employed. This transformation allowed for the conversion of input variables into standard normal variables, preserving their correlation and ensuring suitability for the subsequent FORM analysis aimed at estimating the probability of structural failure.

$$\beta = \frac{\mu_R^N - \mu_D - \mu_L^N}{\sqrt{(\sigma_R^N)^2 + (\sigma_D)^2 + (\sigma_L^N)^2}} \tag{1}$$

The variables involved in these calculations encompassed essential parameters such as μ_R^N (mean value of the resistance normal equivalent variable), μ_D(mean value of the dead load effect variable), μ_L^N(mean value of the live load effect normal equivalent variable), σ_R^N (standard variation of the resistance normal equivalent variable), σ_D (standard variation of the dead load effect variable), and σ_L^N (standard variation of the live load effect normal equivalent variable).

$$p_f = N(-\beta) \tag{2}$$

where:
p_f is the failure probability,
N is the standard normal cumulative distribution function, and
β is the reliability index.

Upon conducting the FORM calculation, as illustrated in Table 2, it appears that the reliability indexes for the Bina Marga standard design for prestressed concrete girder bridges are 3.63. This value falls short of the desired target reliability index of 3.72 [22]. The probability of failure (p_f) was determined using Equation 2, involving the standard normal cumulative distribution function of (– β). The obtained pf amounted to 1.36 x 10^{-4}. This result indicates that the current SNI Bridge Loading Code may result in an under-designed bridge superstructure.

Table 2 Iteration on risk of failure assessment analysis.

Iteration No.	Failure points		σ_L^N	σ_R^N	μ_L^N	μ_R^N	Reliability index (β)	Probability of failure (p_f)
	l*	r*						
1	336.60	1418.06	4.51	198.49	336.57	1404.17	2.91	1.81E-03
2	336.89	842.73	4.51	117.96	336.57	1273.03	3.64	1.38E-04
3	337.15	875.22	4.52	122.51	336.57	1289.00	3.64	1.36E-04
4	337.13	873.22	4.52	122.23	336.57	1288.05	3.64	1.36E-04
5	337.13	873.34	4.52	122.25	336.57	1288.11	3.64	1.36E-04
6	337.13	873.34	4.52	122.24	336.57	1288.11	3.64	1.36E-04
7	337.13	873.34	4.52	122.24	336.57	1288.11	3.64	1.36E-04
8	337.13	873.34	4.52	122.24	336.57	1288.11	3.64	1.36E-04
9	337.13	873.34	4.52	122.24	336.57	1288.11	3.64	1.36E-04
10	337.13	873.34	4.52	122.24	336.57	1288.11	3.64	1.36E-04

The acceptable risk of failure for structures is generally higher for buildings compared to bridges, with a target of 10^{-3} for buildings [23] and 10^{-4} for bridges [24]. This is because bridges are considered more important and critical infrastructure. The results of this study indicate that a standard high-level bridge with a precast prestressed concrete I girder type span of 40 m has a higher risk of failure than the expected target. This is likely due to a variety of influencing factors, including the random and variable nature of the load, which may be different from the loads experienced by bridges in other countries. As such, it is important to carefully consider the unique characteristics of the load on a bridge and ensure that the structure is capable of handling it in order to minimize the risk of failure.

Conclusion

In conclusion, this risk assessment of the standard design for prestressed concrete girder bridges showed that the risk of failure due to live load based on bridge WIM measurements is 1.48 x 10^{-4}. While this value is lower than the acceptable risk of failure for bridges according to the AASHTO LRFD Bridge Design Specification and SNI 1725 2016 (10^{-4}), it is still higher than the expected target for building (10^{-3}). This indicates that there are potentially influencing factors that may increase the risk of failure for this type of bridge. It is important to continue monitoring the performance of this standard designed bridge and consider any necessary measures to improve its reliability and reduce the risk of failure in the future.

In future research, we aim to apply the proposed methodology to a range of standard designed bridges, including various types and span lengths. This expansion is intended to provide a comprehensive understanding of the reliability of existing bridges across Indonesia, considering actual vehicle loading based on B-WIM measurements. By evaluating different bridge designs, our goal is to gain insight into how these structures perform under various traffic conditions. Furthermore, we seek to identify suitable load and resistance factors in line with the Indonesia bridge design code to ensure that the target reliability levels are achieved. This research will play a crucial role in enhancing the safety and reliability of bridge infrastructure throughout the country, adapting to changes in traffic patterns and load distributions.

DOI: 10.5614/j.eng.technol.sci.2023.55.5.5

Acknowledgement

We would like to express our gratitude to the Indonesia Endowment Funds for Education (LPDP) for funding this study and to the Ministry of Public Works and Housing Republic of Indonesia for their support. Without their generosity and support, this research would not have been possible. We are grateful for their commitment to improving infrastructure and ensuring the safety of bridges in Indonesia.

References

[1] Marco, B., Kuo-Chun, C., Tzu-Kang, L. & Nerio, T., *Influence of Prestressing on the Behavior of Uncracked Concrete Beams with a Parabolic Bonded Tendon*, Structural Engineering and Mechanics, **77**(1), pp. 1-17, Jan. 2021. doi: 10.12989/SEM.2021.77.1.001.

[2] Sun, Z., Siringoringo, D.M. & Fujino, Y., *Load-carrying Capacity Evaluation of Girder Bridge using Moving Vehicle*, Engineering Structure, **229**, Feb. 2021. doi: 10.1016/j.engstruct.2020.111645.

[3] Nugraha, W., & Sidi, I. D., *Probability Based Evaluation of Vehicular Bridge Load using Weigh-in-Motion Data*, Journal of Engineering and Technological Sciences, **48**(1), pp. 66-85, Feb. 2016. doi: 10.5614/j.eng.technol.sci.2016.48.1.6.

[4] Bonopera, M., Liao, W.-C. & Perceka, W., *Experimental–theoretical Investigation of the Short-term Vibration Response of Uncracked Prestressed Concrete Members under Long-age Conditions*, Structures, **35**, pp. 260-273, 2022, doi: https://doi.org/10.1016/j.istruc.2021.10.093.

[5] Gan, B. Z., Chiew, S. P., Lu, Y., & Fung, T. C., *The Effect of Prestressing Force on Natural Frequencies of Concrete Beams – A Numerical Validation of Existing Experiments by Modelling Shrinkage Crack Closure*, Journal of Sound and Vibration, **455**, pp. 20-31, Sep. 2019. doi: 10.1016/j.jsv.2019.04.030.

[6] Simanjuntak, V.C., Imran, I., Moestopo, M. & Setio, H.D., *The Evolution of Seismic Design Provisions in Indonesia's National Bridge Code*, Journal of Engineering and Technological Sciences, **54**(6), 220614, Nov. 2022. doi: 10.5614/j.eng.technol.sci.2022.54.6.14.

[7] Mikhail, R., Irsyam, M., Nazir, R., Asrurifak, M., Hutapea, B.M., Rustiani, S., Munirwansyah & Harninto, D.S., *Development of Nationwide Surface Spectral Acceleration Maps for Earthquake Resistant Design of Bridges based on National Hazard Maps of Indonesia 2017*, Journal of Engineering and Technological Sciences, **51**(4), pp. 501-515, Sep. 2019. doi: 10.5614/j.eng.technol.sci.2019.51.4.4.

[8] Directorate General of Highways, *Superstructure Standards for Type I Beam Prestressed Concrete Bridges (Class A) A40,* Indonesia's Ministry of Public Works and Housing, 2008. (Text in Indonesian)

[9] National Standardization Agency, *SNI 1725-2016 Loading for Bridges*, National Standardization Agency, 2016. (Text in Indonesian)

[10] AASHTO, *AASHTO LRFD Bridge Design Specification*, 2012.

[11] Department of Public Works, *Bridge Engineering Planning Regulations,* Department of Public Works, 1992. (Text in Indonesian)

[12] Nowak, A.S., *Live Load Model for Highway Bridges*, Structural Safety, **13**(1), pp. 53-66, 1993. doi: 10.1016/0167-4730(93)90048-6.

[13] Nugraha, W. & Sukmara, G., *Physical Model Test of a Simple Bridge Weigh in Motion System on a Composite Steel Girder Bridge*, Jurnal Jalan-Jembatan, **35**(1), pp. 1-15, 2018. (Text in Indonesian)

[14] Jacob, B. & Feypell-de La Beaumelle, V., *Improving Truck Safety: Potential of Weigh-in-motion Technology*, IATSS Research, **34**(1), pp. 9-15, 2010. doi: 10.1016/j.iatssr.2010.06.003.

[15] Zhao, H., Tan, C., OBrien, E. J., Zhang, B., Uddin, N. & Guo, H., *Developing Digital Twins to Characterize Bridge Behavior Using Measurements Taken under Random Traffic*, Journal of Bridge Engineering, **27**(1), pp. 1-12, 2022. doi: 10.1061/(asce)be.1943-5592.0001814.

[16] Moses, F., *Weigh-in-Motion System Using Instrumented Bridges*, Transportation Engineering Journal of ASCE, **105(**3), pp. 233-249, 1979.

[17] CESTEL & ZAG Institute, *SiWIM Manual,* Ljubljana: CESTEL, 2014.

[18] Computer and Structures Inc., *CSiBridge,* California, Computer and Structures, Inc., 2018.

[19] Lauridsen, J., Bjerrum, J., Sloth, M. & Jensen, F.M., *Principles for a Guideline for Probability-based Management of Deteriorated Bridges*, Proceedings of the 3rd International Conference on Bridge Maintenance, Safety and Management - Bridge Maintenance, Safety, Management, Life-Cycle Performance and Cost, 2006. doi: 10.1201/b18175-205.

[20] Nugraha, W., Sidi, I.D., Suarjana, M. & Zulkifli, E., *Reliability Evaluation of Steel Truss Bridge due to Traffic Load Based on Bridge Weigh-in-motion Measurement*, Structural Monitoring and Maintenance, **9**(4), 323-336, Dec. 2022.

[21] Rosenblatt, M., *Remarks on a Multivariate Transformation*, The Annals of Mathematical Statistics, **23**(3), pp. 470-472, Jun. 1952.

[22] Iatsko, O. & Nowak, A.S., *Revisited Live Load for Simple-Span Bridges*, Journal of Bridge Engineering, **26**(1), pp. 1-14, 2021. doi: 10.1061/(asce)be.1943-5592.0001647.

[23] Sidi, I.D., *Probabilistic Modeling of Seismic Risk-based Design for a Dual System Structure*, Journal of Engineering and Technological Sciences, **49**(2), pp. 179-192, 2017. doi: 10.5614/j.eng.technol.sci.2017.49.2.2.

[24] Nowak, A. & Collins, K., *Reliability of Structures*, Nuclear Instruments and Methods in Physics Research, Section B: Beam Interactions with Materials and Atoms, **259**(1), pp. 359-364, 2007. doi: 10.1016/j.nimb.2007.01.180.

Manuscript Received: 7 March 2023
Revised Manuscript Received: 25 September 2023
Accepted Manuscript: 14 November 2023